

Nature of glassy magnetic state in magnetocaloric materials $Dy_5Pd_{2-x}Ni_x$ ($x = 0$ and 1) and universal scaling analysis of R_5Pd_2 ($R = Tb$, Dy and Er)

Mohit K. Sharma, Gurpreet Kaur and K. Mukherjee

School of Basic Sciences, Indian Institute of Technology, Mandi, Himachal Pradesh -175005, India

Abstract

We report a systematic investigation of the magnetic and magnetocaloric properties of Dy_5Pd_2 and Dy_5PdNi . Our study on these compounds gave evidence that they exhibit complex magnetic behaviour along with the presence of glass-like magnetic phase. Furthermore, in these compounds both second order and first order phase transitions were present, which were validated through Arrott plots and Landau's parameter analysis. AC susceptibility along with time dependent magnetization study has confirmed the presence of double cluster glass-like freezing in both Dy_5Pd_2 and Dy_5PdNi . These compounds show significant value of isothermal entropy change and relative cooling power and these values increased with Ni substitution. Beside conventional magnetocaloric effect, inverse magnetocaloric effect was noted in these compounds, which might arise due to the presence of complex non-equilibrium magnetic state. Along with these compounds a universal characteristic curve involving two other members of R_5Pd_2 family i.e. Er_5Pd_2 and Tb_5Pd_2 was constructed. The master curve reaffirmed the presence of both second and first order magnetic phase transition in such compounds which were in analogy to our results of Arrott plots and Landau's parameter analysis. Additionally, magnetic entropy change followed the power law and the obtained exponent values indicated the presence of mixed magnetic interactions in these compounds.

1. Introduction

Magnetic refrigeration is a highly efficient environment friendly refrigeration technique and it is based on the magnetocaloric effect (MCE) [1-4]. Since last couple of decades, many efforts have been made to explore new magnetocaloric materials which can be used for magnetic refrigeration [1, 5]. Isothermal magnetic entropy change (ΔS_M) and relative cooling power (RCP) are the important parameters to evaluate the magnetocaloric properties of any magnetic material. Magnetic materials having magnetocaloric properties can exhibit either conventional MCE (CMCE) or inverse MCE (IMCE). Negative value of ΔS_M was observed for the former case while a positive value was observed for the later one [6, 7]. CMCE was generally observed for ferromagnet materials [1], while, IMCE had been reported for some antiferromagnetic materials [7]. As per literature reports, many compounds which have second order phase transition (SOPT), show the large MCE and RCP values [1, 5 and 8]. Compounds with first-order phase transition (FOPT) have also been found to exhibit large MCE. However, FOPT provides a narrow ΔS_M peak and generally shows a remarkable thermal/magnetic hysteresis, which reduces the effective RCP [9-11]. On the other hand, compounds with second-order magnetic transition show a good reversible behaviour of MCE. Moreover, some compounds with successive second-order magnetic transitions exhibit ΔS_M distribution over a wide temperature region, and have a large RCP [12-14].

Rare-earth based intermetallic compounds exhibit fascinating magnetic properties along with excellent magnetocaloric properties. In this context, members of R_5Pd_2 series are interesting as they exhibit complex magnetic behaviour along with significant magnetocaloric properties. The magnetic properties of some of the members of R_5Pd_2 series were reported by Klimczak et al. [15]. Large ΔS_M is reported in the compounds Ho_5Pd_2 , Er_5Pd_2 , Tb_5Pd_2 and Dy_5Pd_2 [14, 16-20]. Additionally, complex magnetic behavior and presence of glassy magnetic state were reported for Er_5Pd_2 [19], whereas, double glass transition had been reported for Tb_5Pd_2 [20]. For Dy_5Pd_2 compound a complex cluster glass state had been reported [18]. However there are no reports about whether a second glassy transition is present and also about the nature of the phase transition in this compound. Additionally, there are no detailed studies to see how the physical properties evolve due to partial replacement of Pd.

Hence, in the present manuscript, we carried out an extensive investigation of the magnetic and magnetocaloric properties of Dy_5Pd_2 and Dy_5PdNi . Along with these compounds, we tried to construct the universal characteristic curve of two other members of

R_5Pd_2 family i.e. Er_5Pd_2 and Tb_5Pd_2 in order to check whether this universality holds for different compounds of the R_5Pd_2 family. Our results indicated the presence of double cluster glass-like freezing in Dy_5Pd_2 and Dy_5PdNi . With Ni substitution magnetization, MCE parameters were increased possibly due to the modification of *d-f* exchange interactions. Power law studies on the members of R_5Pd_2 family indicated the presence of mixed magnetic interactions in these compounds. The phenomenological universal curve affirmed the presence of both SOPT and FOPT in such compounds along with the fact that the compounds of this series belong to the same universality class.

2. Experimental details

The polycrystalline compounds Dy_5Pd_2 and Dy_5PdNi were prepared by the arc melting method using stoichiometric amounts of respective high purity elements under similar conditions as reported in [19]. The Tb_5Pd_2 and Er_5Pd_2 compounds were the same as used in Ref [14, 19]. X-ray diffraction (XRD) was performed at room temperature in the range 20° - 70° (steps size 0.02°) using Rigaku smart lab x-ray diffractometer. Figure 1 showed the room temperature indexed X-ray diffraction (XRD) pattern for the compounds Dy_5Pd_2 and Dy_5PdNi . The compounds crystallize in cubic structure and the obtained lattice parameters are tabulated in Table 1. It was observed that with increase in ionic radii of the rare-earth ion the peaks shifted towards lower angle, as noted from the upper inset of Figure 1 (the curves for Tb_5Pd_2 and Er_5Pd_2 were added from Ref [14] and [19] respectively for comparison). This observation substantiates the expansion of lattice with increasing ionic radii of rare earth compounds. Also for Dy_5PdNi the peaks shift to higher angle side in comparison to Dy_5Pd_2 implying that the dopant goes to the respective site (lower inset Figure 1). We also performed the energy dispersive spectroscopy (EDAX) to get confirmation about the average atomic stoichiometry, which was found to be in accordance with the expected values. Magnetic field and temperature dependent magnetization measurements were performed using Magnetic Properties Measurements System and heat capacity measurements were performed using Physical Properties Measurements System, both from Quantum Design, USA.

3. Results and discussion

3.1 Magnetic and MCE studies on $Dy_5Pd_{2-x}Ni_x$ ($x = 0$ and 1)

The dc magnetic susceptibility ($\chi = M/H$) of Dy_5Pd_2 and Dy_5PdNi compounds, were measured under zero field cooling (ZFC) and field cooling (FC) conditions at 100 Oe, as

shown in Figure 2(a). In both compounds a sharp peak was observed and the curves showed a strong bifurcation below the peak temperature. This type of feature was also observed for other members of R_5Pd_2 series [14, 18-19]. For Dy_5Pd_2 this aspect was ascribed to paramagnetic to glass-like freezing (around 38 K). In Dy_5PdNi the peak temperature shifted to the higher temperature side (around 39.5 K) (Figure 2(a)) and it showed slightly enhanced magnetic properties as compared to Dy_5Pd_2 . The inverse magnetic susceptibility (χ^{-1}) of these compounds follows the Curie-Weiss law ($\chi^{-1} = (T - \theta_p)/C$) above 75 K (inset Figure 2(a)). The obtained effective moment (μ_{eff}) and the Curie Weiss temperature (θ_p) are tabulated in Table 1. The positive value of θ_p suggests the dominance of ferromagnetic like interactions. Additionally magnetic moment value was also increased with the substitution. This observed enhancement could be ascribed to the magnetic nature of the Ni atom, i.e. Ni at Pd site provides additional magnetic contribution along with rare earth atom. Actually, when Ni was substituted at Pd site of Dy_5Pd_2 , *d-f* exchange interaction got modified, which possibly resulted in an increment of magnetic ordering and magnetization value.

In order to further understand the magnetic nature of compound, magnetic isotherms as a function of applied field (in the range ± 70 kOe) at different temperatures (2-100 K) were measured and the resulting curves are shown in Figure 2(b). It is noted that M (H) isotherms do not saturate up to the highest applied field (70 kOe) and show hysteresis at lower temperature. The former is the property of systems with finite antiferromagnetic coupling, whereas the presence of later property is an indication of the existence of ferromagnetic component, implying that multiple interactions were present in these compounds. Similar behaviour had also been reported in literature for other compounds [20]. Additionally coercive field was found to decrease exponentially with increasing the temperature for both the compounds (lower inset Figure 2(b)). Furthermore it was also observed that in these compounds no long ranged magnetic ordering was present, as was observed from the temperature response of heat capacity, which, do not show any peak (upper inset Figure 2(b)) in the temperature range of measurement. These results also supported the presence of glass-like behaviour in these compounds which were also in accordance to the results obtained for other R_5Pd_2 members [14, 19-20].

In order to investigate the nature of magnetic phase transition in both the compounds, Arrott plots studies were carried out. Figure 2 (c) and (d) shows the H/M vs M^2 plots obtained by using the virgin isothermal magnetization curves. According to the Banerjee's criterion, the slopes of Arrott plots were used to distinguish between the FOPT and SOPT. The observation of negative slope was an indication for FOPT while the presence of positive

slope was a signature for SOPT [21]. As noted from the figure, a positive slope was observed near to the peak temperature while a negative slope was observed at lower temperature, which indicated towards SOPT and FOPT respectively. Therefore, from the Arrott plots studies it can be said that, there is a possibility of the presence of two types of phase transition in these compounds. To confirm the exact temperature, we analyzed the Arrott plots' data in terms of magnetic free energy $F(M, T)$. Landau's expansion of free energy, can be expressed as [22]; $F(M, T) = C_1 M^2/2 + C_3 M^4/4 + C_5 M^6/6 + \dots -HM$; where $C_1(T)$, $C_3(T)$ and $C_5(T)$ were the Landau coefficients. These coefficients were calculated by using the equation [13, 22]; $H/M = C_1(T) + C_3(T) M^2 + C_5(T) M^4$. The sign of coefficient C_3 determines the order of phase transition; for the negative value, the transition is FOPT, while, it is a SOPT for the positive value of C_3 . The calculated value of C_3 is plotted as function of temperature (inset Figure 2 (c)-(d)). The curve shows positive value at 17 K for Dy_5Pd_2 and 18 K for Dy_5PdNi . For each compound, C_3 changed its sign below this temperature, which was in accordance to our observation of slope change from Arrott plots. From the above analysis, it was noticed that both FOPT and SOPT were present in the Dy_5Pd_2 and Dy_5PdNi compounds.

In both the compounds a strong irreversibility between ZFC and FC magnetization and absence of any peak in heat capacity indicated the presence of glass-like freezing. Also the ZFC curves showed a weak and a broad feature below 20 K. Hence in order to confirm the possibility of a second transition and the presence of glassy magnetic phase in these compounds, ac susceptibility measurement at different frequencies was performed. In order to do ac susceptibility measurements, the compounds was cooled from paramagnetic region to lowest measured temperature in zero dc field, then measurement had been performed at different frequencies of 13, 131, 531 and 931 Hz in presence of 1 Oe ac field. It is to be noted that the real part of ac susceptibility has already been reported in Ref [18]. For both compounds the temperature dependent real (χ') and imaginary (χ'') parts of ac susceptibility were measured, are shown in Figure 3(a-d). For Dy_5Pd_2 , the χ' curve (at 13 Hz) showed a peak at 38 K (T_1) along with a weak hump-like behaviour at low temperature. Interestingly, χ'' curve (at 13 Hz) showed two frequency dependent distinct peaks, one at T_1 and other around 14 K (T_2). However for Dy_5PdNi , these peaks were shifted upwards to 39.5 and 16 K respectively. Both the peaks were frequency dependent and shifted upwards with increasing frequency, which is a characteristic of glassy systems. These frequency dependent temperature peaks were analysed by the Mydosh parameter; $\delta T_f = [\Delta T_f / (T_f (\Delta \log f))]$; along with power law behaviour, $\tau = \tau_0 (T_f / T_g - 1)^{-z\nu}$, where τ_0 represents the relaxation time of

single spin flip, zv is the exponent, T_g represents the true glass transition temperature and T_f is the frequency dependence of this glass transition temperature [23]. The scaled relaxation time τ as function of reduced temperature $\varepsilon = [(T_f/T_g - 1)]$ for both peaks are shown in the insets I of Figure 3. The obtained fitting parameters are shown in the table 2. In the spin glass system δT_f varies from 0.005 to 0.01 and $\tau_0 \sim 10^{-13}$ sec, whereas for a cluster glass system δT_f varies from 0.02 to 0.06 and a much slower relaxation rate has been observed [23, 24]. The observed value of zv lies in the range to that observed for different kinds of glassy system [25, 26]. The values of the obtained parameters around T_1 suggested cluster glass behaviour of both the compounds. The peak at T_2 (as shown in Figure 3 (b) and (d)) possibly originated due to the presence of another complex non-equilibrium magnetic state. The fitted parameters (as tabulated in Table 2) also indicated that this peak aroused due to an additional cluster glass freezing. Around this peak, δT_f was found in the range, which was reported for cluster glasses; however, τ_0 was much higher, which indicated that the cluster size increased on decreasing the temperature. This increment in cluster size might be responsible for the non-equilibrium magnetic behavior present in the compounds. The difference in δT_f and τ_0 values indicated that the size and average distribution of the cluster were changed around both the peaks. To further substantiate the spin dynamics in Dy_5Pd_2 and Dy_5PdNi , we analyzed the ac susceptibility data by Arrhenius law, $\tau = \tau_0 \exp(E_a/k_B T_f)$, where τ_0 represents the characteristic relaxation time, k_B is the Boltzmann constant and E_a is the average thermal activation energy. The resulting curve in terms of $\ln(\tau)$ as a function of $(1/T)$ were shown insets II of the Figure 3 (a), (b) for Dy_5Pd_2 and (c), (d) for Dy_5PdNi . Both the compounds showed nonlinear behavior around T_1 and T_2 . This non-linear behavior indicated that the spin dynamics in both the compounds might arise due to the interacting clusters rather than individual spin. In order to give further evidences about the presence of double cluster glass behaviour in these compounds, we have calculated the Tholence parameter $\delta T_{Th} = (T_f - T_0)/T_f$, where T_0 is Vogel-Fulcher (V-F) temperature and T_f is peak temperature at frequency 13 Hz [27]. T_0 was obtained by fitting the ac magnetization data by Vogel-Fulcher (V-F) law (not shown) [14, 23]. The values of this parameter (Table 1) obtained for both compounds around T_1 and T_2 , are in analogy to that observed for other cluster glass systems [28, 29], implying the presence of double cluster glass behaviour in both of these compounds. The glass-like magnetic state in such type of cubic system has also been reported in Tb_5Pd_2 , where glassiness is explained in terms of atomic disorder [20].

In order to investigate the non-equilibrium magnetic state at low temperature, the magnetic relaxation measurement was performed. The following protocol was used for the time response of magnetization: the compound was cooled in a zero field from a temperature in paramagnetic region to the measuring temperature (5 and 20 K). Once the measurement temperature was reached, a magnetic field of 50 Oe was applied for 20 min. After that the field was switched off and magnetization was noted as function of time (Figure 4(a)). From the results of both the compounds, it was noticed that the magnetization showed decaying nature with time and decay rate was more at low temperature. Generally for compounds which undergo long ranged magnetic ordering, magnetization remains unchanged with time. Our results gave another strong indication of the presence of glassy phase and absence of long ranged order magnetic phase in these compounds. The data was fitted using the equation; $M = M_0 - S \ln(1 + t/t_0)$; where M_0 is a parameter and S is the magnetic viscosity [30]. For Dy_5Pd_2 and Dy_5PdNi , the obtained fitting parameters are shown in table 2. The logarithmic relaxation implies that the distribution of energy barrier in these systems arises due to the presence of different types of spin clusters. Our experimental results suggested the existence of the collective relaxation behaviour in these compounds. Additionally, the M_0 and S showed decreasing value with decreasing temperature which indicated that both compounds showed an additional glass-like freezing at low temperature [14]. Moreover, with the Ni substitution, both were increased, which was analogous to the magnetization results.

As per literature reports, members of R_5Pd_2 series, including Dy_5Pd_2 showed large MCE [14, 18 and 19]. In order to check the changes in MCE properties due to Ni substitution, MCE for both the compounds was calculated in terms of the isothermal magnetic entropy change (ΔS_M). The ΔS_M was calculated from the virgin curve of $M(H)$ isotherms and each of these curves was measured after cooling the respective compounds from room temperature to the measurement temperature. ΔS_M was calculated from the Maxwell's thermodynamic relation i.e. $(\partial S/\partial H)_T = (\partial M/\partial T)_H$, where the symbols have their usual meaning [1]. Generally, in the SOPT region a conventional magnetocaloric effect was observed, while, an inverse magnetocaloric effect was observed in the FOPT region [16, 31]. Fig 4 (b)-(c) shows the temperature response of ΔS_M for both the compounds. The observed values of ΔS_M of both the compounds are tabulated in table 1. As observed from the figure, the curves showed a broad peak around the temperature which is far above the magnetic transition temperature. Therefore the magnetic cooling commenced from the peak

temperature of ΔS_M verses T curve. This effect was maximum around 55 K and below this temperature, ΔS_M showed decreasing behavior and become zero around 30 K in the presence of 20 kOe field. As the temperature was further decreased, an IMCE was observed and the result shows the heating effect instead of cooling under the same refrigeration cycle. The appearance of CMCE with IMCE in the same compounds can find a possible application in magnetic cooling/heating based constant temperature bath [32]. Additionally, the large ΔS_M was noted in the temperature range where the magnetic hysteresis was absent, thereby fulfilling another important condition for a magnetic refrigerant material. Generally, for long-ranged ordered magnetic material, a symmetric temperature evolution of ΔS_M has been reported [1]. However for this case an asymmetric curve was observed and ΔS_M was found to be distributed over a large temperature range. Such behavior arises due to the presence of short-ranged magnetic interactions which are also responsible for the observed glassy behavior. In these compounds, the cluster glass nature and inter and intra cluster magnetic interactions might be responsible for the observed IMCE in the low temperature region of these compounds. The crossover in low temperature region also indicated the presence of two types of phase transition in these compounds [31], which was also in analogy to the observation of Arrott plots and Landau's parameter study.

In order to check the practical utility of any compound which can be used as magnetic refrigerant, the RCP is calculated as it is the measure of the amount of heat transfer between cold and hot reservoir in an ideal refrigeration cycle. It is defined as the product of maximum of ΔS_M (ΔS_M^{max}) and full width of half maximum of the peak in ΔS_M (ΔT_{FWHM}) [33], i.e. $RCP = \Delta S_M^{max} \times \Delta T_{FWHM}$; where $\Delta T_{FWHM} = T_h - T_c$, T_c and T_h are the temperatures corresponding to half maximum value of ΔS_M peak value around both the side. The RCP values of these compounds were calculated (Table 1). It is noted that the with the Ni substitution both ΔS_M and RCP values had increased significantly. This result has certain practical significance considering the high price of Pd metal. Hence it can be said that with substitution of Ni at Pd site, MCE parameters can be increased, implying that Ni substitution can tune the value of MCE in a positive way.

3.2 Universal scaling analysis and power law study of R_5Pd_2

In order to have a better understanding of MCE properties of magnetic compounds a phenomenological universal curve was also constructed. Universal scaling and power law are extensively used to characterize the MCE in magnetic compounds [34-38]. They are the key tools which allow us to compare the performing properties of the compounds regardless of their nature, processing or experimental conditions during measurement. If a universal curve

exists, then all points of ΔS_M curves measured at different applied fields should merge into a single master curve. The MCE data of different compounds of same universal class should fall onto the same curve; however the magnitude of the applied magnetic field does not matter. These curves also gave the information about nature of magnetic phase transitions [39]. For symmetric behavior of ΔS_M curve, generally, universal scaling has been done without rescaling the temperature (as peak temperature and ordering temperature have nearly same value). However, in case of asymmetric behavior of ΔS_M curve, we need to rescale the temperature axis around the peak temperature of ΔS_M [34, 38 and 39]. The universal curve in terms of normalized ΔS_M and reduced temperature (θ) was constructed for Dy_5Pd_2 and Dy_5PdNi . Along with these compounds we constructed the curve of two other members of R_5Pd_2 family i.e. Er_5Pd_2 and Tb_5Pd_2 on the same graph in order to check whether this universality is held for different compounds of the R_5Pd_2 family. The MCE behavior of the latter two compounds have already been reported in literature [14, 19], and the values of ΔS_M were taken from these references. The above exercise was performed by using the following expression: $\theta = ((T - T_{pk})/(T_r - T_{pk}))$; where, T_{pk} is temperature at peak value of ΔS_M and T_r is the reference temperature, greater than T_{pk} , where ΔS_M has its half value. Figure 5(a)-(d) exhibits the normalized ΔS_M as function of θ for R_5Pd_2 series of compounds. The universal curve holds for all studied compounds with single reduced temperature. At low temperatures (below the peak of ΔS_M), the normalized ΔS_M curves were not fully merged which gave indications of presence of FOPT. This result was analogous to our Arrott plots study. Around the peak temperature and above it the universality are completely held, i.e. all curves were merged and showed similar critical behavior irrespective of applied field and temperature. This also confirmed the presence of SOPT in the studied compounds. Moreover, the universal curve merged into single master curve (inset of Figure 5(a)) for R_5Pd_2 , which suggested that the compounds of this series along with Dy_5PdNi show similar universality and in all these compounds, SOPT as well as FOPT were present.

Also, ΔS_M depends both on temperature and applied magnetic field. The applied field response of the magnitude of ΔS_M was characterized in terms of power law ($\Delta S_M \sim H^n$), where n is the exponent and directly related with the magnetic state of the compounds [37]. For a ferromagnetic compound obeying Curie Weiss law, the value of n is 1 in the ferromagnetic state. However, in the paramagnetic region and antiferromagnetic ordered state, the value of n is 2 [40-42]. At $T = T_C$, $n \sim 0.66$ for those compounds which obey the mean field theory. For the present case, these compounds show features of a glassy magnetic system along with the presence of inhomogeneous magnetic state at low temperature. Additionally, it is to be noted

that the peak temperatures in ΔS_M verses T and M verses T plots, do not match perfectly. It has already been reported in literature, that it is not necessary for both the temperatures to perfectly match with each other and this matching is possible only in those compounds which follow the mean field theory [40, 43]. Therefore, to extract the nature of magnetic state, investigation of applied field dependence of ΔS_M is another useful tool. This exercise was performed on the studied compounds in the field range 0 to 40 kOe and representative curves at selected temperatures are shown in Figure 5(e-h). The analysis of field response of the magnitude of ΔS_M was done in the three temperature regime; first paramagnetic region (above T_1), second around T_1 and third is around T_2 . The ΔS_M verses T curve follows the power law behavior in the paramagnetic region and observed values of n are found to lie in between 1.3 to 2. Hence, the true paramagnetic regions for these compounds (except Er_5Pd_2) lie far above the glass freezing, like for Tb_5Pd_2 above 120 K, above 40 K, Dy_5Pd_2 above 70 K and Dy_5PdNi above 75 K. Around the T_1 , the value of n is different for different rare earth like; for Tb_5Pd_2 , Er_5Pd_2 , Dy_5Pd_2 and Dy_5PdNi the values of n are 3.7, 1.1, 3.4 and 2.3 respectively. These values are quite high and indicated that R_5Pd_2 series of compounds does not follow the mean field theory. Additionally, nature of glassy phase was different for different rare earth which was in accordance to previous reports of R_5Pd_2 . As per literature reports, power law does not hold for the field induced and/or inhomogeneous magnetic state [44]. Around T_2 , where ΔS_M has changed its sign, the compounds do not follow the power law behavior with field implying the presence of temperature and applied field dependent inhomogeneous magnetic phase below T_1 .

4. Conclusion

In summary, a comprehensive study on the magnetic and magnetocaloric properties of the Dy_5Pd_2 and Dy_5PdNi was carried out. Our results pointed towards the absence of long range magnetic ordering and observation of double cluster glass-like freezing in both compounds. These materials have good MCE properties and an increment in these properties with Ni substitution was noted. With Ni substitution magnetization, ΔS_M and RCP were increased possibly due to the modification of $d-f$ exchange interactions. Additionally, along with CMCE, IMCE was also observed at lower temperatures in both the compounds. A phenomenological universal curve for these compounds along with Er_5Pd_2 and Tb_5Pd_2 was generated by normalizing the entropy change with rescaled temperature. This master curve affirmed the presence of both SOPT and FOPT in such compounds which were in analogy to the results of Arrott plots and Landau's parameter analysis. The ΔS_M verses H curve was found to follow power law and the result indicated the presence of mixed magnetic

interactions in these compounds. Our studies of universal curve and power law behavior of applied field response of ΔS_M clearly indicate that the compounds of this series belong to the same universality class.

Acknowledgements

The authors acknowledge the experimental facilities of Advanced Materials Research Center (AMRC), IIT Mandi. Financial support from the SERB project EMR/2016/00682 is also acknowledged.

References

- [1] A.M. Tishin and Y.I. Spichkin, *The Magnetocaloric Effect and its Applications* (2003), Institute of Physics Publishing, Bristol
- [2] V.K. Pecharsky and K.A. Gschneidner Jr., *Magnetocaloric effect and magnetic refrigeration*, J. Magn. Magn. Mater. 200 (1999), pp. 44-56.
- [3] E. Bruck, *Developments in magnetocaloric refrigeration*, J. Phys. D. Appl. Phys. **38** (2005), pp.R381.
- [4] X. Moya, V. Kar-Narayan and N.D. Mathur, Nat. Mater. **13** (2014), pp.439.
- [5] K.A. Gschneider Jr., V.K. Pecharsky, A.O. Tsokol, Reports Prog. Phys. **68** (2005), pp.1479.
- [6] T. Krenke, E. Duman, M. Acet, E.F. Wassermann, X. Moya, L. Mañosa and A. Planes, Nat. Mater. **4** (2005), pp.450–454.
- [7] A. Biswas, T. Samanta, S. Banerjee and I. Das, Appl. Phys. Lett. **94** (2009), pp.233109.
- [8] Ling-Wei Li, Chin Phys. B 25 **3** (2016), pp.037502.
- [9] N.H. Duc and D.T.K. Anh, J. Magn. Magn. Mater. **873** (2002), pp.242-245.
- [10] J. Liu, T. Gottschall, K.P. Skokov, J.D. Moore and O. Gutfleisch, Nature Mater. **11** (2012), pp.620.
- [11] Yan Zhang, Qiaoyan Dong, Xinqi Zheng, Yanli Liu, Shulan Zuo, Jie Fu Xiong, Bo Zhang, Xin Zhao, Rui Li, Dan Liu, Feng-xia Hu, Jirong Sun, Tongyun Zhao and Baogen Shen, AIP Advances **8** (2018), pp.056418.
- [12] Lingwei Li, Katsuhiko Nishimura, Wayne D Hutchison, Zhenghong Qian, Dexuan Huo and Takahiro Namiki, Appl. Phys. Lett. **100** (2012), pp.152403.
- [13] S. Pakhira, C. Mazumdar, R. Ranganathan, S. Giri and M. Avdeev, Phys. Rev. B **94** (2016), pp.104414.
- [14] Mohit K. Sharma and K. Mukherjee, J. Magn. Magn. Mater **466** (2018), pp.317-322.
- [15] M. Klimczak, E. Talik, A. Winiarski and R. Troc, J. Alloys and Compounds **423** (2006), pp.62.
- [16] T. Samanta, I. Das and S. Banerjee, Appl. Phys. Lett. **91** (2007), pp.082511.
- [17] S. Toyoizumi, H. Kitazawa, Y. Kawamura, H. Mamiya, N. Terada, R. Tamura, A. Donni, K. Morita and A. Tamaki, J. Appl. Phys. **117** (2015), pp.17D101.
- [18] T. Paramanik, T. Samanta, R. Ranganathan and I. Das, RSC Adv. **5** (2015), pp.47860.
- [19] Mohit K Sharma, Kavita Yadav and K. Mukherjee, J. Phys. Condens. Matter. **30** (2017), pp.215803.
- [20] A.F. Gubkin, E.A. Sherstobitova, P.B. Terentyev, A. Hoser and N.V. Baranov, J. Phys. Cond. Mat. **25** (2013), pp.236003.

- [21] S.K. Banerjee, Phys. Lett. **12** (1964), pp.16.
- [22] Sachin B. Gupta and K.G. Suresh, Appl. Phys. Lett. **102** (2013), pp.022408.
- [23] J.A. Mydosh, “*Spin Glasses: An Experimental Introduction*”, Taylor and Francis, London (1993).
- [24] Y. Sun, M.B. Salamon, K. Garnier and R.S. Averback, Phys. Rev. Lett. **91** (2003), pp. 167206.
- [25] V.K. Anand, D.T. Adroja, A.D. Hillier, Phys. Rev. B **85** (2012), pp.014418; M.H. Phan, N.A. Frey, H. Srikanth, M. Angst, B.C. Sales and D. Mandrus, J. Appl. Phys. **105** (2009), pp.07E308.
- [26] J.F. Gomez-Gracia, R. Escudero and G. Tavizon, J. Solid State Chem. **217** (2014), pp.42-49.
- [27] J.L. Tholence, *Recent experiments about the spin glass transition*, Phys. B (Amsterdam) **126** (1984), pp.157.
- [28] S. Mukherjee, R. Ranganathan, P.S. Anilkumar and P.A. Joy, Phys. Rev. B **54** (1996), pp.13.
- [29] O.F. de Lima, J.A.H. Coaquirra, R.L. de Almeida and S.K. Malik, J. App. Phys. **107** (2010), pp. 09E107.
- [30] D.X. Li, S. Nimori, Y. Shiokawa, Y. Haga, E. Yamamoto and Y. Onuk, Phys. Rev. B **68** (2003), p.012413.
- [31] Julia Lyubina, J. Phys. D: Appl. Phys. **50** (2017), pp.053002.
- [32] S.M. Yusuf, Amit Kumar, and J.V. Yakhmi, Appl. Phys. Lett **95** (2009), pp.182506.
- [33] M-H Phan, S-C Yu, J. Magn. Magn. Mater. **308** (2007), pp.325–340.
- [34] Mohit K. Sharma and K. Mukherjee, J. Magn. Magn. Mater. **444** (2017), pp.178–183.
- [35] A. Biswas, S. Chandra, T. Samanta, M.H. Phan, I. Das and H. Srikanth, J. Appl. Phys. **113** (2013), pp.17A902.
- [36] V.Franco and A. Conde, Int. J. Refrigeration **33** (2010), pp.465.
- [37] V. Franco, J.S. Blázquez and A. Conde, Appl. Phys. Lett. **89** (2006), pp.222512.
- [38] V. Franco, J.S. Blázquez and A. Conde, J. Appl. Phys. **103** (2008), pp.07B316.
- [39] C.M. Bonila, J.H. Albillos, F. Bartolome, L.M. Garcia, M.P. Borderias and V. Franco, Phys. Rev. B **81** (2010), pp.224424.
- [40] V. Franco, J.S. Blázquez and A. Conde, J. Appl. Phys. **100** (2006), pp.064307.
- [41] A. Biswas, S. Chandra, T. Samanta, B. Ghosh, S. Datta, M.H. Phan, A.K. Raychaudhuri, I. Das and H. Srikanth, Phys. Rev. B **87** (2013), pp.134420.
- [42] S. Chandra, A. Biswas, T. Samanta, B. Ghosh, S. Datta, A.K. Raychaudhuri and H. Srikanth, Nanotechnology **24** (2013), pp.505712 (9pp).
- [43] H. Oesterreicher and F.T. Parker, J. Appl. Phys. **55** (1984), pp.4334.
- [44] T.D. Shen, R.B. Schwarz, J.Y. Coulter and J.D. Thompson, J. Appl. Phys. **91** (2002), pp.15.

Table 1. Fitted and calculated parameters for the studied compounds; Lattice parameter (a), calculated effective magnetic moment (μ_{eff}), Curie-Weiss temperature (θ_p), isothermal magnetic entropy change (ΔS_M) and relative cooling power (RCP)

Compounds	$a(\text{\AA})$	μ_{eff} (μ_B)	θ_p (K)	ΔS_M (J/kg-K) For 70 kOe	RCP (J/kg) For 70 kOe
Dy ₅ Pd ₂	13.527	11.59	40	-6.8	405
Dy ₅ PdNi	13.422	11.64	47	-9	570

Table 2. The fitting parameter obtained from ac susceptibility and time dependent magnetization measurement

	Mydosh parameter		Power law fitting						Tholence parameter			
	T_1 (K)	T_2 (K)	$\delta T_f(T_1)$	$\delta T_f(T_2)$	T_{g1} (K)	T_{g2} (K)	τ_{01} (s)	τ_{02} (s)	zv_1	zv_2	$\delta T_{\text{Th}}(T_1)$	$\delta T_{\text{Th}}(T_2)$
Dy ₅ Pd ₂	38	14	0.018 ± 0.003	0.087 ± 0.04	35.5	8	7.2×10^{-11}	3.1×10^{-4}	7.45 ± 0.48	7.13 ± 0.4	0.12	0.53
Dy ₅ PdNi	39.5	16.5	0.017 ± 0.004	0.065 ± 0.02	37.5	16	7×10^{-10}	4.6×10^{-5}	6.31 ± 0.4	2.14 ± 0.03	0.11	0.12
Time dependent fitting parameter												
	Dy ₅ Pd ₂			Dy ₅ PdNi								
T (K)	5		20		5		20					
S (emu/g m)	0.0017 ± 0.0001		0.0056 ± 0.0001		0.0026 ± 0.0003		0.0027 ± 0.0001					
M_0 (emu/gm)	0.0165 ± 0.0001		0.0499 ± 0.0002		0.0327 ± 0.0002		0.0235 ± 0.0001					
t_0 (sec)	2.63 ± 0.26		9.82 ± 0.36		2.57 ± 0.25		12.95 ± 0.37					

List of figures

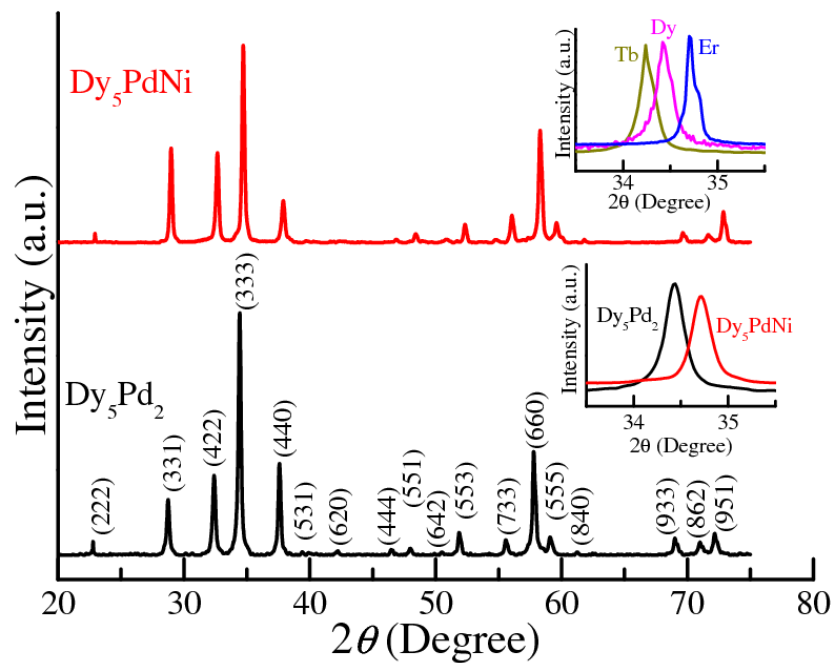


Figure 1. Room temperature X-ray diffraction pattern (XRD) for Dy_5Pd_2 and Dy_5PdNi . Upper Inset: XRD pattern in an expanded form for one peak for the series R_5Pd_2 , to bring out that the peaks shift with different rare earth (Tb, Dy and Er). Lower Inset: The enlarged view of XRD pattern of Dy_5Pd_2 and Dy_5PdNi for seeing the effect of Ni substitution.

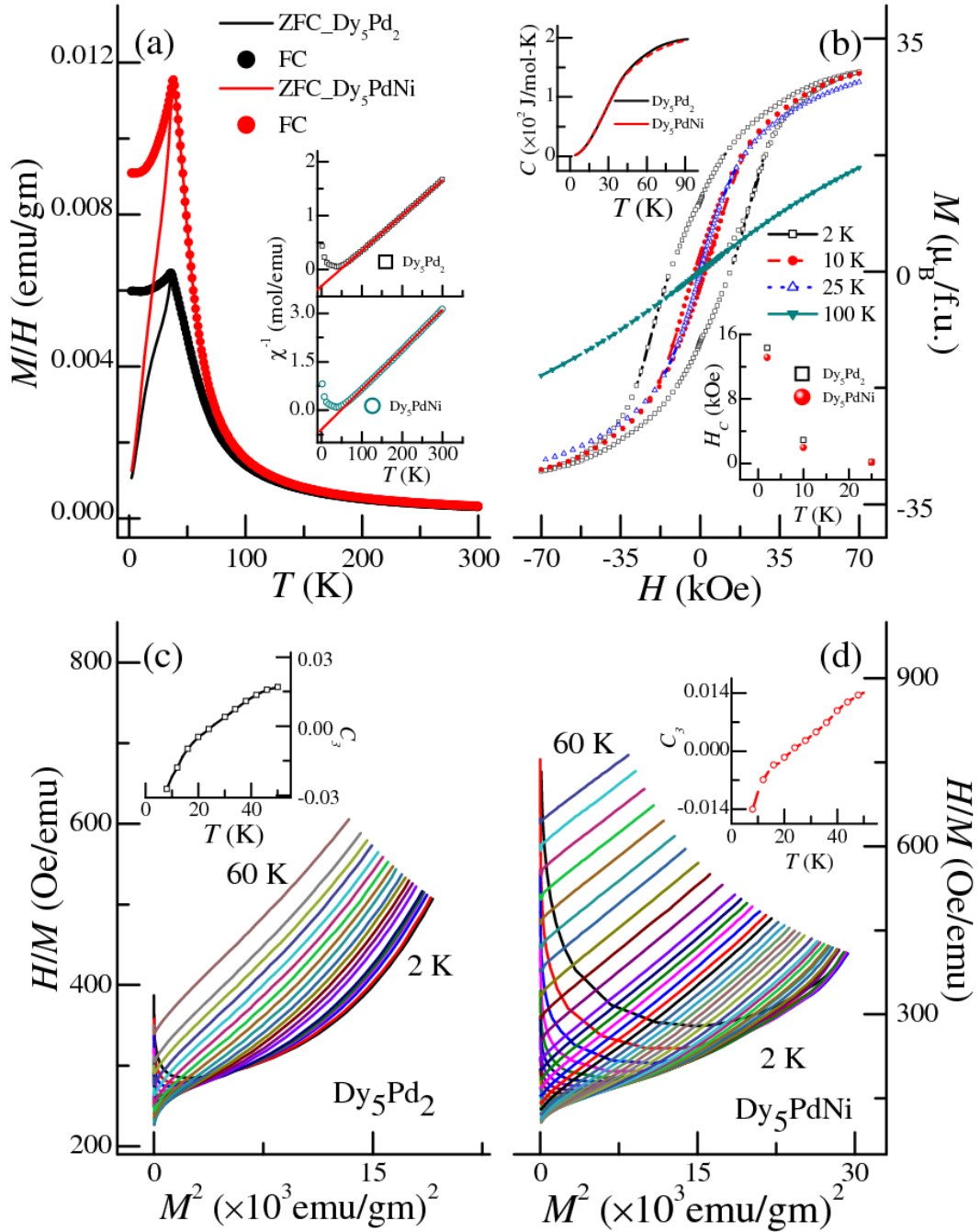


Figure 2. (a) Zero field cooling (ZFC) and field cooling (FC) magnetization as a function of temperature at 100 Oe for Dy_5Pd_2 and Dy_5PdNi . Inset shows the Curie-Weiss law for Dy_5Pd_2 and Dy_5PdNi . (b) Magnetic isotherms at selected temperatures for Dy_5PdNi . Upper inset: Heat capacity as a function of temperature for Dy_5Pd_2 and Dy_5PdNi . Lower inset: Coercive field versus temperature plot for Dy_5Pd_2 and Dy_5PdNi . (c) and (d) H/M versus M^2 curves for Dy_5Pd_2 and Dy_5PdNi respectively. Insets: Landau parameter (C_3) as function of temperature for the respective compounds.

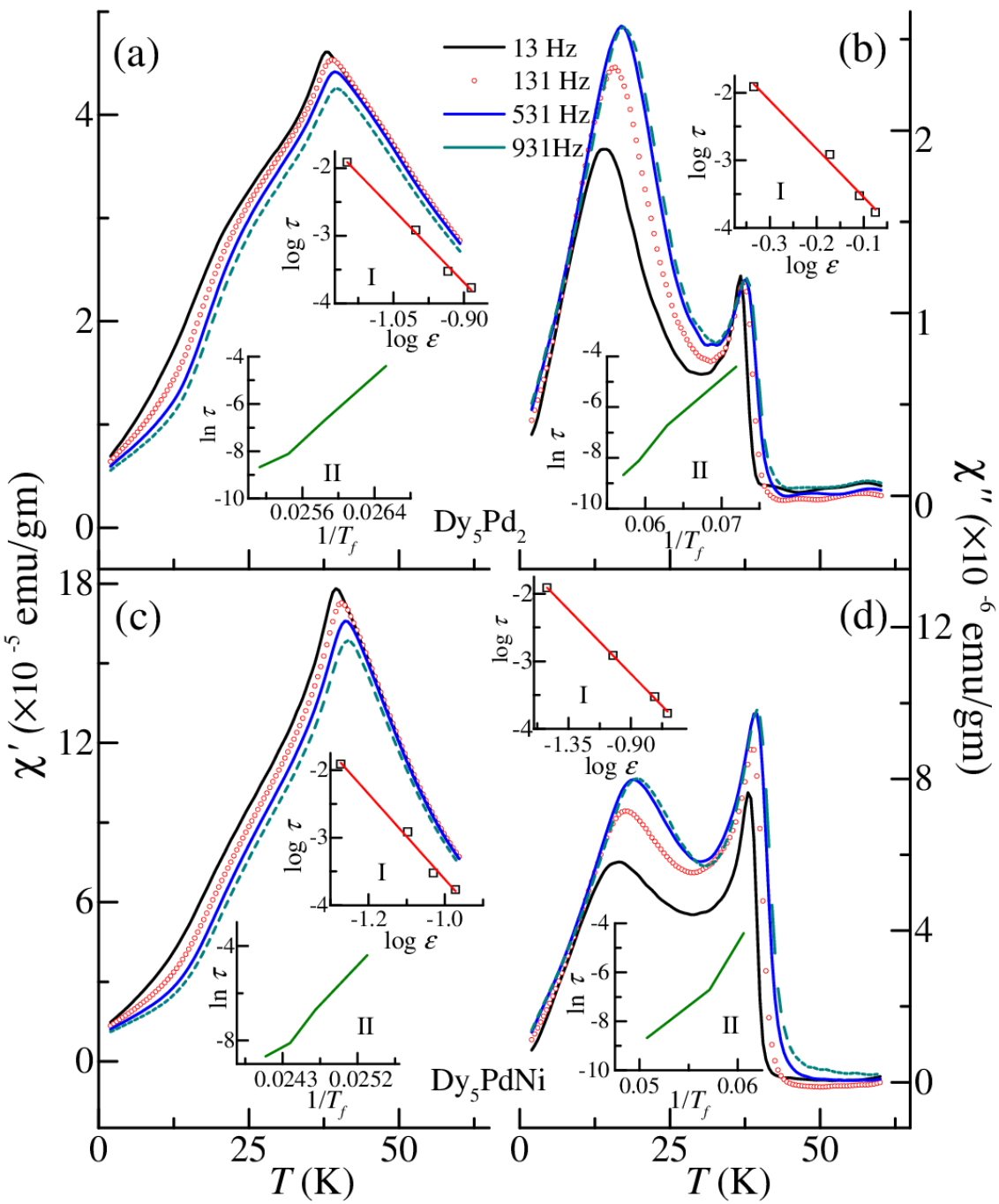


Figure 3. (a) and (c) Temperature response of real part of ac susceptibility for Dy₅Pd₂ and Dy₅PdNi respectively. (b) and (d) Temperature response of imaginary part of ac susceptibility for Dy₅Pd₂ and Dy₅PdNi respectively. Inset I: Power law fitting for the respective peak temperature. Inset II: Arrhenius plot for the respective peak temperature.

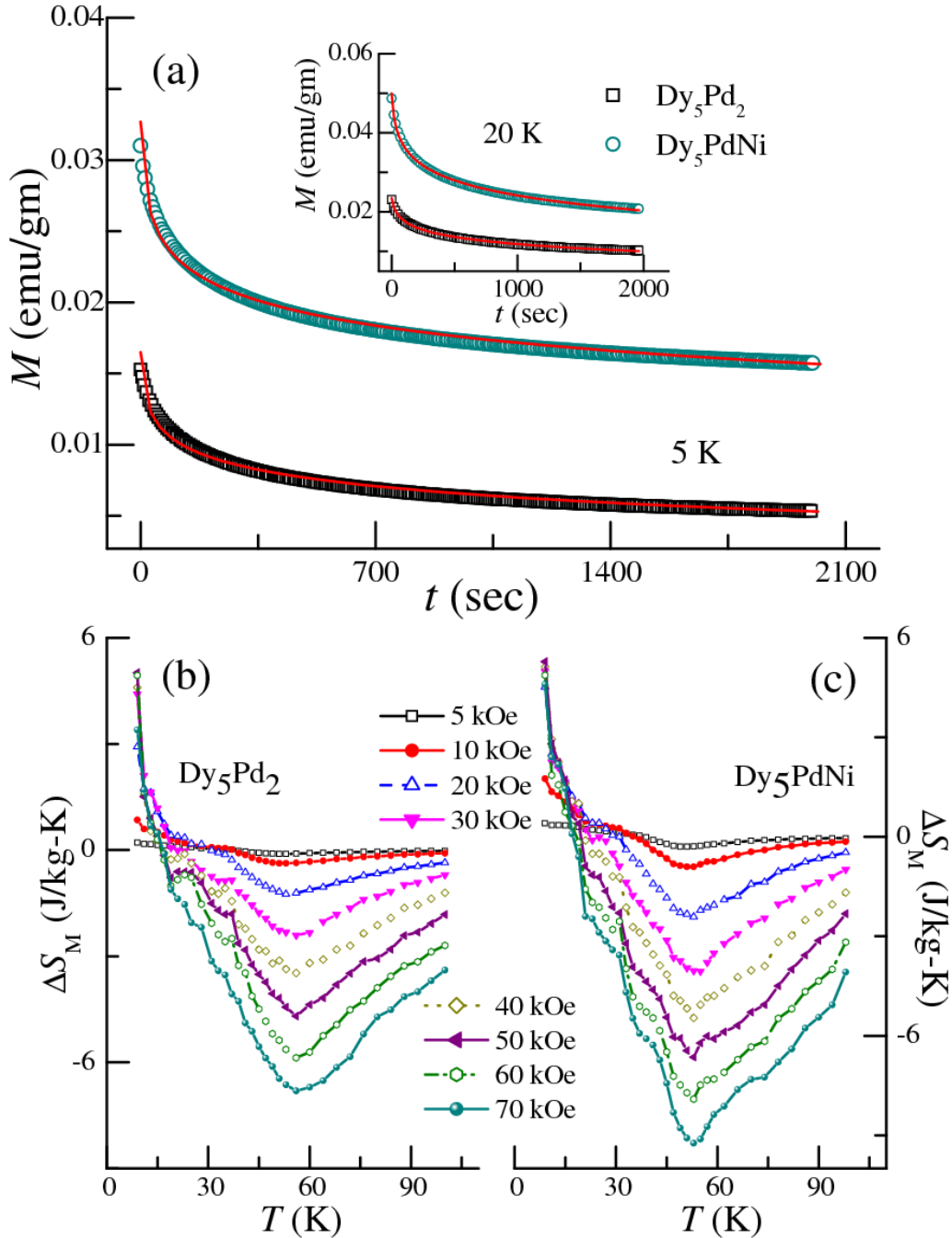


Figure 4. (a) Time response of magnetization for Dy_5Pd_2 and Dy_5PdNi at 5 K. Inset shows the similar plot at 20 K. Solid red lines represents the logarithmic fitting using equation $M = M_0 - S \ln(1 + t/t_0)$. (b) and (c) Temperature response of isothermal magnetic entropy change (ΔS_M) for Dy_5Pd_2 and Dy_5PdNi respectively.

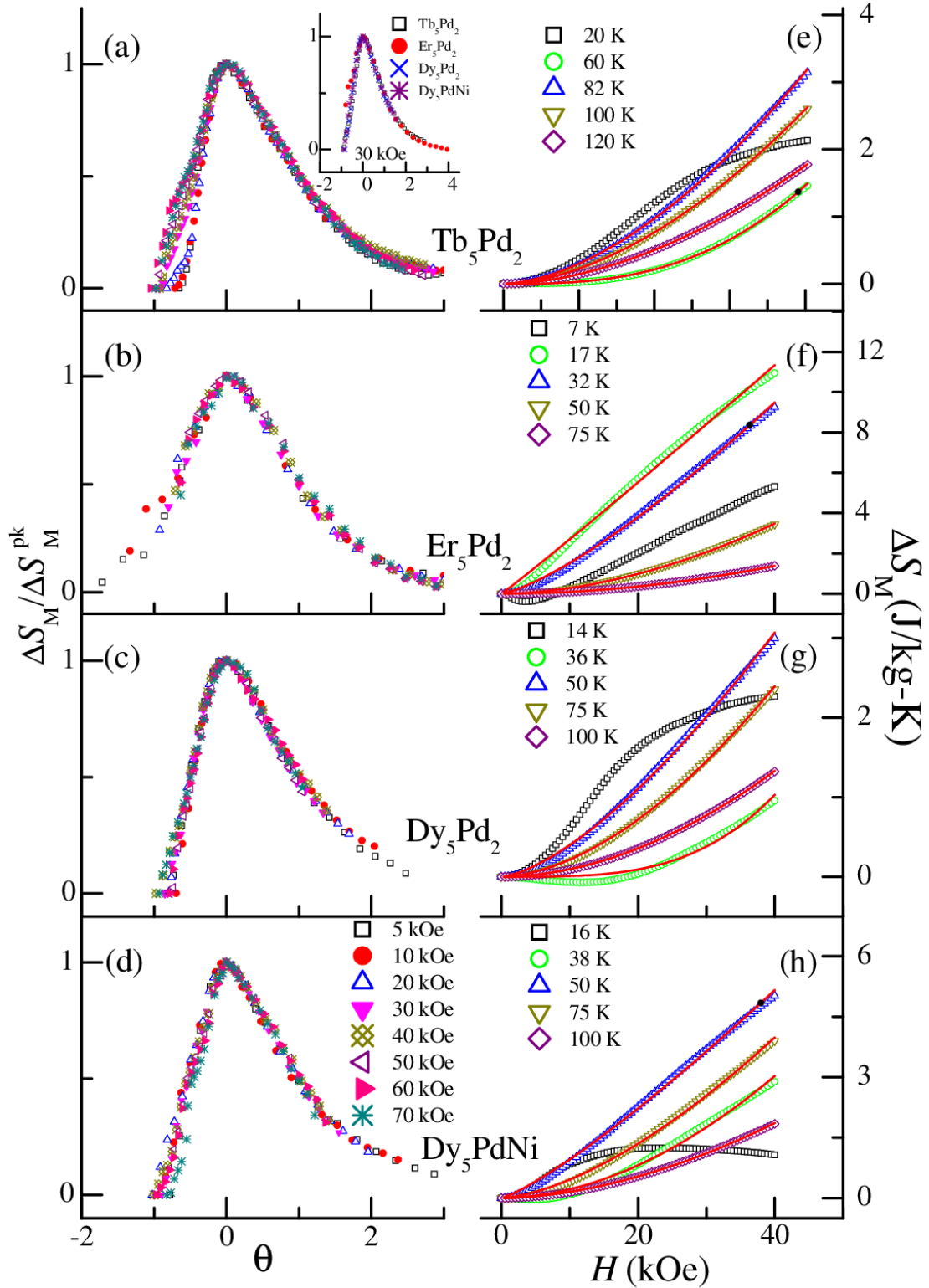


Figure 5. Left panel: Reduced temperature (θ) response of normalized ΔS_M : (a) Tb_5Pd_2 , (b) Er_5Pd_2 , (c) Dy_5Pd_2 , and (d) Dy_5PdNi . Inset of (a) shows the universal plot for all the compounds. Right panel: Magnetic field response of ΔS_M at selected temperatures for (e) Tb_5Pd_2 , (f) Er_5Pd_2 , (g) Dy_5Pd_2 and (h) Dy_5PdNi . The solid red lines through the curves represent the power law fitting.